

# Cold Dust in Kepler's Supernova Remnant.

H.L.Morgan<sup>1</sup>, L.Dunne<sup>1</sup>, S.A.Eales<sup>1</sup>, R.J.Iverson<sup>2</sup>, M.G.Edmunds<sup>1</sup>

## ABSTRACT

The timescales to replenish dust from the cool, dense winds of Asymptotic Giant Branch stars are believed to be greater than the timescales for dust destruction. In high redshift galaxies, this problem is further compounded as the stars take longer than the age of the Universe to evolve into the dust production stages. To explain these discrepancies, dust formation in supernovae (SNe) is required to be an important process but until very recently dust in supernova remnants has only been detected in very small quantities. We present the first submillimeter observations of cold dust in Kepler's supernova remnant (SNR) using SCUBA. A two component dust temperature model is required to fit the Spectral Energy Distribution (SED) with  $T_{warm} \sim 102\text{K}$  and  $T_{cold} \sim 17\text{K}$ . The total mass of dust implied for Kepler is  $\sim 1M_{\odot}$  - 1000 times greater than previous estimates. Thus SNe, or their progenitors may be important dust formation sites.

*Subject headings:* ISM: abundances—dust, supernova: individual—Kepler

## 1. Introduction

Recent blank field submillimeter (submm) surveys and observations of distant quasars have discovered a population of extremely dusty objects at high redshifts (Smail, Ivison & Blain 1997; Bertoldi et al. 2003) implying that large quantities of dust are present in the Universe at  $z > 4$  (Eales et al. 2003; Ivison et al. 2003, Issak et al 2002). Dust is generally believed to form in the cool atmospheres of giant stars and expelled via slow dense winds, yet at these redshifts, the time needed for such a process is greater than the age of the Universe. Morgan & Edmunds (2003) constructed models of the maximum dust mass produced in high redshift galaxies. Using a simple method to estimate the condensation efficiency of dust in

---

<sup>1</sup>Department of Physics and Astronomy, University of Wales Cardiff PO Box 913, CF24 3YB; haley.morgan@astro.cf.ac.uk

<sup>2</sup>Astronomy Technology Centre, Royal Observatory, Blackford Hill, Edinburgh EH9 3HJ

Stellar Winds (SW's) they found there is not enough time at redshifts  $> 4$  for significant amounts of dust to be made in SW's unless star formation rates are *very* high and dust destruction rates are low. Dust production in SNe however provides an explanation for the dust seen in high redshift SCUBA sources as SNe evolve on a much shorter timescale.

Theoretical models of nucleation of dust grains in supernova gas suggest condensation efficiencies of  $\sim 0.1$  (Clayton, Deneault & Meyer 2001) and  $\sim 0.2 - 0.8$  (Todini & Ferrara 2001) could be reached in Type II SNe regardless of initial metallicity. However, the observational evidence that SNe produce large quantities of dust is very weak. Infra-Red (IR) observations of young SNRs with IRAS and ISO found only  $\sim 10^{-3}$  and  $10^{-4}M_{\odot}$  of dust in Tycho and Kepler (Douvion et al. 2001b) and  $10^{-4}M_{\odot}$  in Cas A (Douvion, Lagage & Pantin 2001a; Arendt, Dwek & Moseley 1999). Observations of SN1987A have found a similar amount of dust (Dwek et al. 1992; Wooden 1997) although this could be much higher if the ejecta is clumpy (Lucy et al. 1991). One possible reason for the discrepancy between observations and theory would be if the dust in the SNRs is cold and virtually impossible to detect at IR wavelengths but observable in the submm waveband. Recent SCUBA observations of Cas A (Dunne et al. 2003) have shown that a colder population of grains does exist with an estimated  $2 - 4M_{\odot}$  of dust, which implies a condensation efficiency of  $0.5 - 0.8$  for a  $30M_{\odot}$  progenitor star. In this Letter, we present the first submm observations of another young Galactic SNR, Kepler's SNR.

Kepler's SNR is the remnant from the early 1600's (Green 2001). Recent estimates place it at a distance of 4.8 - 6.4kpc (Reynoso & Goss 1999) so we adopt 5kpc. The progenitor and type of Kepler's SN are still hotly debated. It was originally thought to be a Type Ia SN due to its light curve, and its distance from the Galactic plane suggests the progenitor was an old population II object. However, slow moving optical knots present in the region around the SNR show substantial overabundance of nitrogen, which can be most naturally explained by the the CNO cycle in massive stars (Bandiera 1987; Borkowski, Blondin & Sarazin 1992). The slow expansion velocity and high densities of the knots suggest they were not ejected in the SN explosion but rather in an earlier stellar wind, which again suggests a massive star progenitor (Blair, Long & Vancura 1991). X-Ray models of the remnant provide further evidence for a dense medium. These require ambient densities of a few H atoms per cubic centimeter (Kinugasa & Tsunemi 1991), which is 100 times greater than the ambient density of the interstellar medium (ISM) expected at 600pc above the Galactic plane (Whittet 2001). All these observations indicate there was dense circumstellar material (CSM) predating the SNR, which is most easily explained by the stellar winds from a massive star. For these reasons, Kepler's supernova has been classified as a Type Ib SN. Bandiera (1987) has proposed that the progenitor of Kepler's SNR was a massive star which was ejected from the galactic plane. In this model, the star moves through its own stellar

wind, compressing the wind material into a bow shock in the direction of motion, and this produces the N-S asymmetry seen in the X-Ray and radio observations.

## 2. Data Reduction

We observed Kepler’s SNR with SCUBA at the 15m James Clerk Maxwell Telescope (JCMT) on Mauna Kea in Hawaii. SCUBA simultaneously observes at 450 and 850 $\mu\text{m}$  using bolometer arrays of 91 and 37 bolometers respectively. The field of view (fov) is  $\sim 2.3$  arcmin, but is slightly smaller at 450 $\mu\text{m}$ . The beam size (FWHM) at these wavelengths is  $\sim 8$  and 15 arcsecs respectively. As Kepler’s SNR is actually larger than the fov of SCUBA, we observed the remnant with six ‘jiggle-map’ observations, each jiggle map being centered around the SNR with a chop throw of 180 arcsec.

The data was reduced using the SURF software package (Sandell et al. 2001). We made corrections for atmospheric absorption using the opacities derived from skydip measurements with the JCMT and from polynomial fits to the sky opacity measured by the Caltech Submillimeter Observatory at 225GHz. Noisy bolometers were flagged and large spikes were removed. Any noise correlated across the array (i.e sky noise) was removed using the SURF program REMSKY. A map was made from the six individual datasets using one-arcsec pixels. We created noise maps at each wavelength using the Monte-Carlo technique described in Eales et al. (2000). The S/N images at 850 and 450 $\mu\text{m}$  are shown in Figure 1 with the 850 $\mu\text{m}$  map clearly showing a ring like morphology similar to the X-Ray and radio observations. The 450 $\mu\text{m}$  map shows emission in both the north-western and south-eastern quadrant. The noise at 450 $\mu\text{m}$  has a much stronger dependence on the atmospheric conditions than the noise at 850 $\mu\text{m}$ . The conditions were much worse when we observed the other two quadrants, so the lack of obvious emission in those quadrants and also in the centre of the remnant may partly be the result of the increased noise in these regions.

The image was calibrated using primary calibrators which were observed with similar chop throw to the observations of the SNR. The flux was measured in eight apertures, which were placed on the maps to include all the obvious emission from the SNR (using the S/N maps as a guide). The flux calibration was carried out using apertures of the same size on the calibrator map. The errors in the fluxes were estimated as described in Dunne et al. (2000) with calibration errors of 15% and 20% respectively. The fluxes measured over the whole remnant at 850 and 450 $\mu\text{m}$  are  $1.0 \pm 0.2\text{Jy}$  and  $3.0 \pm 0.7\text{Jy}$  respectively. Thus the ratio of 450 to 850 $\mu\text{m}$  flux for the SNR as a whole is 3.

### 3. Estimating the Dust Mass

Supernova remnants are strong sources of synchrotron radiation which can contaminate the longer submm wavelengths. To obtain the submm flux which is emitted by dust grains only, we need to correct for this contamination. Using the average of the IR fluxes from the literature (Arendt 1989; Saken, Fesen & Shull 1992; Braun 1997) and the submm fluxes from this work, we can produce Kepler’s IR-Radio SED (Figure 2). This clearly shows that the emission from dust is in excess of the synchrotron emission. We can estimate the contribution of the synchrotron to the submm using the five radio measurements which are well fitted by a power law slope  $S_\nu \propto \nu^\alpha$  where  $\alpha = -0.71$ . Hence the synchrotron emission is responsible for 30% of the submm flux at  $850\mu\text{m}$  and 6% at  $450\mu\text{m}$ .

Comparison of the 450 and  $850\mu\text{m}$  maps with a radio map also clearly indicates that there is submillimetre emission in excess of the expected synchrotron emission. Figure 1(c) shows the 5GHz VLA image of the SNR (Delaney, private communication). The map shows the well known N-S asymmetry associated with the interaction with a dense CSM. The  $850\mu\text{m}$  map also shows a N-S asymmetry but is much less pronounced than the radio. The  $450\mu\text{m}$  map shows an even lesser N-S asymmetry. A point-by-point comparison of the maps also indicates excess submm emission. The strong emission visible in the south west on the submm maps is at a position where there is hardly any emission on the radio map.

To correct the submm images for the contribution of synchrotron radiation we smoothed the VLA radio image to the resolution of the submm images and scaled it to the submm wavelengths using the power law spectrum shown in Figure 2. We then subtracted it from the submm image. The synchrotron-subtracted  $850\mu\text{m}$  image is shown in Figure 1(d). The brighter northern limb in the  $850\mu\text{m}$  unsubtracted image has been removed and the 450 and  $850\mu\text{m}$  images now follow a similar morphology with two bright emission regions in the north and south of the remnant. The peaks on the 450 and  $850\mu\text{m}$  maps do not exactly coincide with each other but this is not unexpected given the low S/N at  $450\mu\text{m}$  and the fact that we are extrapolating a long way in frequency from 5GHz to the submm waveband. The remnant is known to have variations in the spectral index of order  $\pm 15\%$  (Delaney et al. 2002). This may produce errors in the synchrotron-corrected maps although the general agreement between the 450 and  $850\mu\text{m}$  images suggests this is not a problem. Note also that the fact that the ratio of 450 to  $850\mu\text{m}$  is 3 makes it practically impossible to explain the excess submm emission by some synchrotron process.

The dust mass can be measured directly from the flux at submm wavelengths using  $M_d = \frac{S_\nu D^2}{\kappa_\nu B_\nu(\nu, T)}$  (Hildebrand, 1983) where  $S_\nu$  is the flux density measured at frequency  $\nu$ ,  $D$  is the distance and  $\kappa_\nu$  is the dust mass absorption coefficient.  $B$  is the Planck function and  $T$  is the dust temperature. We tried fitting a single temperature greybody to the SED

( $S_\nu \propto B_\nu \nu^\beta$ ) but we could not obtain an acceptable fit. So we fitted a two-temperature greybody allowing  $\beta$  and the warm and cold temperatures to vary. The best fit SED gave  $\beta = 1.2$ ,  $T_w = 102K$  and  $T_c = 17K$ . The possible reasons why the dust could be so cold are discussed in Dunne et al (2003) and will be considered in future work (Dunne et al, in prep). We cannot rule out the presence of dust existing at intermediate temperatures between these two extremes until further observations around the peak of the SED ( $200\mu\text{m}$ ) are made. We used a bootstrap technique to derive errors on these values. We created 3000 sets of artificial fluxes from the original data and then fit our two temperature model to each set. We derived our errors from the distribution of  $T_w$ ,  $T_c$  and  $\beta$  produced by these fits.

The largest uncertainty in the dust mass comes from the uncertainty in  $\kappa$ . We have followed Dunne et al. (2003) in trying three different values of  $\kappa$  from the literature: (1)  $\kappa_{850} = 0.6 - 1.1m^2kg^{-1}$ , the range observed in laboratory studies of clumpy aggregates. (2)  $\kappa_{850} = 0.16 - 0.8m^2kg^{-1}$  the range observed in circumstellar environments/reflection nebulae and (3)  $\kappa_{850} = 0.04 - 0.15m^2kg^{-1}$ , the range observed for the diffuse ISM where dust is likely to have encountered extensive processing. In each case we used the average values of the ranges to estimate the dust mass which are given in Table 1. In Cas A, the higher  $\kappa$  values were required to give a reasonable dust mass. Using the highest  $\kappa$  values for Kepler gives a lower range of  $0.2 - 0.3M_\odot$  whereas using the lowest  $\kappa$  values gives  $1 - 3M_\odot$ . Whichever value of  $\kappa$  we use we obtain at least three orders of magnitude more dust than obtained from mid-IR measurements. This is an order of magnitude lower than the dust observed in Cas A but the far greater brightness of Cas A than Kepler at all wavelengths implies a (as yet not understood) difference in the dynamics of the explosions.

#### 4. Discussion

Kepler’s SNR still appears to be in an early evolutionary phase in which the swept up mass is not much more than the total ejected mass (Dickel 1987; Hughes 1999). If the interstellar density at the location of Kepler’s SNR is  $n_H \sim 0.001 - 0.1cm^{-3}$  (Bandiera 1987; Borkowski et al. 1992) then given the size of the remnant and assuming a normal gas to dust ratio of 160, the maximum dust mass swept up by the SNR is  $\sim 10^{-3}M_\odot$ .

Evidence for an even denser CSM comes from slow moving optical knots observed outside of the ejecta. These are thought to originate from accelerated clumps of circumstellar material and have densities  $n_H \sim 1000cm^{-3}$ , which imply a pre-shock density of  $100cm^{-3}$  (Blair et al. 1991). If this density is representative of the CSM surrounding the entire remnant, then the blast wave could have swept up  $100M_\odot$  of gas and a dust mass of  $\sim 1M_\odot$ . This is however, at odds with the mass observed in the X-Ray which suggests that there is

only  $\sim 2 - 5M_{\odot}$  of gas within the SNR (Kinugasa & Tsunemi 1991; Borkowski et al. 1992).

Some additional arguments that the dust has not been swept up come from considering the morphologies of the different images. Some of the dust is found between the forward and reverse shocks of the X-Ray gas, where the gas is thought to be dominated by the ejecta rather than the swept up material (Hughes 1999). A large fraction of the dust is also found in the south of the SNR, where the radio image shows no evidence for a strong interaction between the SNR and a dense CSM. However, some of the submm emission is found outside the X-Ray and Radio remnants. This may be due to some of the dust being formed in the progenitor’s stellar wind or due to the velocity of the ejecta moving faster in these regions. The lack of a detailed position for the two shock fronts does not allow for a complete comparison though further work will try to address this problem (Dunne et al, in prep).

Could the dust be from a massive star, formed in its pre-supernova RSG and WR phases? The maximum observed dust mass lost in WR winds is  $6 \times 10^{-7}M_{\odot}yr^{-1}$  (Marchenko et al. 2002). The violent mass loss from the WR will blow the material outwards into a shell with outer radius depending on the velocity and duration of the wind. If the wind velocity is  $\sim 1000kms^{-1}$  and if the WR wind was responsible for the dust seen at the radius of the submm emission, the WR phase of the precursor must have only lasted around  $10^4$  years. This would produce only  $0.01M_{\odot}$  of dust. The interaction between the previous RSG and WR winds may have created more dust but the maximum yield of heavy elements ejected from the most massive stars during the RSG phase is  $< 2M_{\odot}$ . The condensation efficiency in these atmospheres was estimated to be  $< 10\%$  (Morgan & Edmunds 2003) and hence it is difficult to produce all of the observed dust in this way. Note, if the condensation efficiency is indeed higher, this *could* explain the lower end of the cold dust mass in Kepler and hence SNe progenitors would be responsible for polluting the high redshift galaxies.

The mass of dust we observe is lower but similar to the mass of dust found in Cas A. If Kepler’s progenitor was a  $30M_{\odot}$  star (Bandiera 1987), the condensation efficiency could have been  $\sim 0.1 - 0.6$ . If we assume that the dust in Kepler’s SNR is representative of the dust formed in every  $30M_{\odot}$  progenitor then this is roughly comparable with the dust mass/SNe given in Todini & Ferrara (2001). Using their models with the condensation efficiency obtained for Kepler’s SNR from this work, we estimate that SNe inject  $\sim 5 - 15(\times 10^{-3})M_{\odot}yr^{-1}$  into the ISM. If the dust injection rate for giant stars is  $\sim 5(\times 10^{-3})M_{\odot}yr^{-1}$  (Whittet 2001; Morgan & Edmunds 2003) then SNe are injecting around 1 - 3 times more dust than stellar winds. Adding supernova or massive stars as a source of dust to the Galactic interstellar medium explains the high redshift submm observations and could well resolve the current discrepancy (Jones et al. 1994) between dust production and destruction rates.

HM would like to acknowledge a Cardiff University studentship and LD is supported by a PPARC postdoctoral fellowship. We would also like to thank Tracey Delaney for providing the radio image and Eli Dwek for useful discussions. We thank the referee for invaluable comments on the draft manuscript.

## REFERENCES

- Arendt, R.G., 1989, *ApJS*, 70, 189
- Arendt, R.G., Dwek, E., Moseley, S.H., 1999, *ApJ*, 521, 234
- Bandiera, R., 1987, *ApJ*, 319, 885
- Bertoldi, F., Carilli, C., Cox, P., Fan, X., Strauss, M.A., Beelen, A., Omont, A., Zylka, R., 2003, *A & A*, 406, L55
- Blair, W.P., Long, K.S., Vancura, O., 1991, *ApJ*, 366, 484
- Borkowski, K.J., Blondin, J.M., Sarazin, C.L., 1992, *ApJ*, 400, 222
- Braun, R., 1987, *A & A*, 171, 233
- Clayton, D.D., Denault, E.A.N., Meyer, B.S., 2001, *ApJ*, 562, 480
- Delaney, T., Koralesky, B., Rudnick, L., Dickel, J.R., 2002, *ApJ*, 580, 914
- Dickel, J.R., Sault, R., Arendt, R.G., Matsui, Y., Korista, K.T., 1987, *ApJ*, 330, 254
- Douvion, T., Lagage, P.O., Pantin, E., 2001a, *A & A*, 369, 589.
- Douvion, T., Lagage, P.O., Cesarsky, C.J., Dwek, E., 2001b, *A & A*, 373, 281
- Dunne, L., Eales, S.A., Ivison, R.J., Morgan, H.L., Edmunds, M.G., 2003, *Nature*, 424, 285.
- Dunne, L., Eales, S., Edmunds, M.G., Ivison, R., Alexander, P., Clements, D.L., 2000, *MNRAS*, 315, 115
- Dwek, E., Mosely, S.H., Glaccum, W., Graham, J.R., Loewenstein, R.F., Silverberg, R.F., Smith, R.K., 1992, *ApJ*, 389, L21
- Eales, S., Lilly, S., Webb, T., Dunne, L., Gear, W., Clements, D., Yun, M., 2000, *AJ*, 120, 2244
- Eales, S., Bertold, F., Ivison, R., Carilli, C.L., Dunne, L., Owen F., 2003, *MNRAS*, 344, 169
- Green, D.A., 2001, *A Catalogue of Galactic Supernova Remnants*, Mullard Radio Astronomy Observatory, Cavendish Laboratory, Cambridge, U.K.
- Hildebrand, R.H., 1983, *Quart.J.Roy.Astron.Soc.*, 24, 267
- Hughes, P., 1999, *ApJ*, 527, 298



- Isaak, K., Priddey, R.S., McMahon, R.G., Omont, A., Peroux, C., Sharp, R.G., Witthington, S., 2002, MNRAS, 329, 149
- Iverson et al, 2002, MNRAS, 337, 1
- Jones, A.P., Tielens, A.G.G.M., Hollenbach, D.J., McKee, C.F., 1994, ApJ, 433, 797
- Kinugasa, K., Tsunemi, H., 1991, PASJ, 51, 239
- Lucy, L.B., Danziger, I.J., Gouiffes, C., Bouchet, P., 1991, *in* Supernovae, The Tenth Santa Cruz Workshop in Astronomy and Astrophysics, eds Woosley, S.E., p.82, Springer-Verlag, New York
- Marchenko, S.V., Moffat, A.F.J., Vacca, W.D., Côté, S., Doyon, R., 2002, ApJ, 565, L59
- Matsui, Y., Long, K.S., Dickel, J.R., Greisen, E.W., 1984, ApJ, 287, 298
- Morgan, H.L., Edmunds, M.G, 2003, MNRAS, 343, 427.
- Reynoso, E.M. & Goss, W.M., 1999, AJ, 118, 926
- Saken, J.M., Fesen, R.A., Shull, J.M., 1992, ApJS, 81, 715
- Sandell, G., Jessop, N., Jenness, T., 2001, SCUBA Map Reduction Cookbook, starlink cookbook 11.2
- Smail, I., Iverson, R.J., Blain, A.W., 1997, ApJL, 490, L5
- Todini, P., & Ferrara, A., 2001, MNRAS, 325, 726
- Whittet, D.C.B., 2001, Dust in the Galactic Environment, IOP, Cambridge University Press, UK
- Wooden, D., 1997, *in* Astrophysical Implications of the Laboratory Study of Presolar Materials, eds. T.J.Bernatowicz & E.K.Zinner, AIP Conference, 402, 317

Table 1: The parameters from the SED fitting using minimum  $\chi^2$  fit to the points. The dust masses are the median of the distribution from the bootstrap technique (same as the best fit values) with 68% confidence interval quoted as the error. The values of  $\kappa$  are (as in Dunne et al. 2003)  $\kappa_1(450) = 1.5m^2kg^{-1}$ ,  $\kappa_1(850) = 0.76m^2kg^{-1}$  (laboratory studies);  $\kappa_2(450) = 0.88m^2kg^{-1}$ ,  $\kappa_2(850) = 0.3m^2kg^{-1}$  (observations of evolved stars);  $\kappa_3(450) = 0.26m^2kg^{-1}$ ,  $\kappa_3(850) = 0.07m^2kg^{-1}$  (observations of the diffuse ISM).

Parameters			Dust Mass ( $M_\odot$ )		
$\beta$	$T_h$ (K)	$T_c$ (K)	$\kappa_1$	$\kappa_2$	$\kappa_3$
$1.2 \pm 0.4$	$102 \pm 12$	$17^{+3}_{-2}$	$M_{450} = 0.3^{+0.2}_{-0.1}$	$0.5^{+0.3}_{-0.2}$	$1.7^{+0.9}_{-0.61}$
			$M_{850} = 0.3 \pm 0.1$	$0.6 \pm 0.2$	$2.7^{+0.6}_{-0.5}$

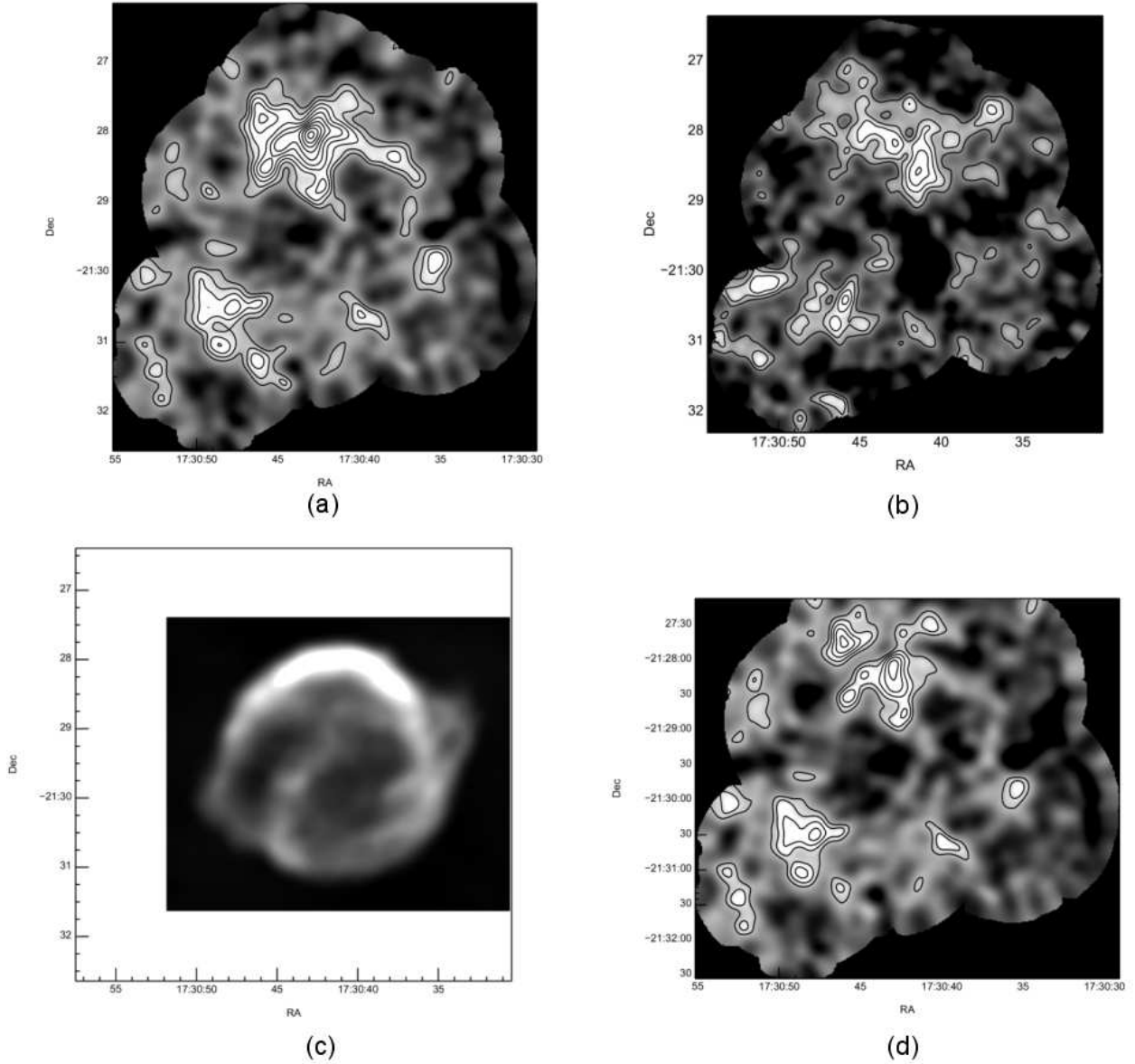


Fig. 1.— Signal/Noise maps of the Kepler SNR. (a)  $850\mu\text{m}$  smoothed to  $14''$  with contours  $3\sigma$ ,  $4\sigma$ ,  $5\sigma$ ...etc. (b)  $450\mu\text{m}$  image smoothed to the  $850\mu\text{m}$  resolution with contours  $1.5\sigma$ ,  $2.5\sigma$ ,  $3.5\sigma$ ... (c) 6cm radio image of Kepler (Delaney et al. 2002) smoothed to the resolution of the  $850\mu\text{m}$  beam. (d) The synchrotron subtracted  $850\mu\text{m}$  image with levels showing  $3\sigma$ ,  $4\sigma$ ,  $5\sigma$ ...

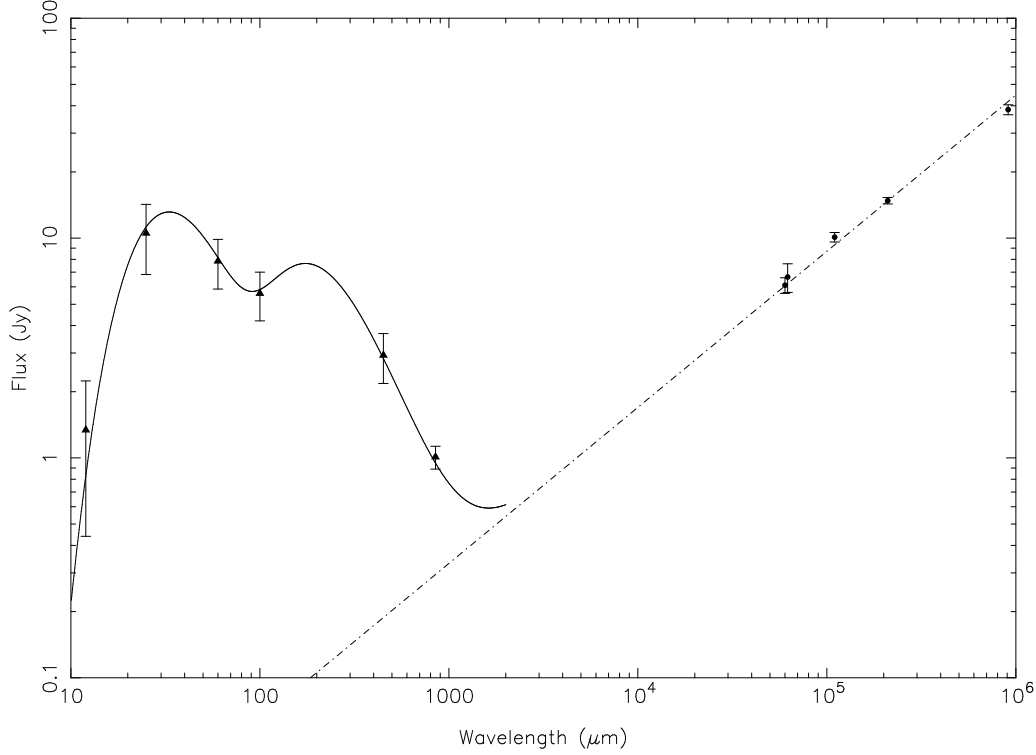


Fig. 2.— Kepler’s IR - Radio SED for the IRAS 12, 25, 60 and 100 $\mu\text{m}$  fluxes, the 850 and 450 $\mu\text{m}$  measurements from this work and the radio (Matsui et al. 1984; Delaney et al. 2002). The solid line represents a two temperature fit to the data points with  $\beta = 1.2$ ,  $T_w = 102K$ ,  $T_c = 17K$ . The straight line through the radio measurements is a power law with a spectral index -0.71. The 100 $\mu\text{m}$  flux was chosen here to be 5Jy rather than the lower value of  $\sim 3\text{Jy}$  observed by Arendt (1989) and Braun (1987). This was a conservative choice as using the lower value would produced a more pronounced second peak in the SED. To obtain the best fit greybody through these points would then require a cold temperature of  $\sim 11K$  and hence more than double the derived dust mass.